Sigdel, Shalik Ram; Zheng, Xiangyu; Babst, Flurin; [et al.]. «Accelerated succession in Himalayan alpine treelines under climatic warming». Nature Plants, Vol. 10 (December 2024), p. 1909–1918.

Accelerated succession in Himalayan alpine treelines under climatic warming

Shalik Ram Sigdel[a], Xiangyu Zheng[a,b], Flurin Babst[c,d], J. Julio Camarero[e], Shan Gao[a], Xiaoxia Li[a], Xiaoming Lu[a], Jayram Pandey[a,b], Jian Sun[a], Haifeng Zhu[a], Tao Wang[a], Eryuan Liang[a,1], Josep Peñuelas[f,g],

[a]State Key Laboratory of Tibetan Plateau Earth System, Environment and Resources (TPESER), Institute of Tibetan Plateau Research, Chinese Academy of Sciences, Beijing 100101, China
[b]University of Chinese Academy of Sciences, Beijing 100049, China
[c]School of Natural Resources and the Environment, University of Arizona, Tucson, AZ 85721, USA
[d]Laboratory of Tree-Ring Research, University of Arizona, Tucson, AZ 85721, USA
[e]Instituto Pirenaico de Ecología (IPE-CSIC), Zaragoza 50059, Spain
[f]CREAF, Cerdanyola del Valles, Barcelona 08290, Spain
[g]CSIC, Global Ecology Unit CREAF-CSIC-UAB, Barcelona, Spain

[1]To whom correspondence may be addressed.
Dr. Eryuan Liang
State Key Laboratory of Tibetan Plateau Earth System, Environment and Resources (TPESER), Institute of Tibetan Plateau Research, Chinese Academy of Sciences, Beijing 100101, China
Email: liangey@itpcas.ac.cn
Phone No: +86 010-84097069

Abstract

Understanding how climate change influences succession is fundamental for predicting future forest composition. Warming is expected to accelerate species succession at their cold thermal ranges, such as alpine treelines. Herein we examined how interactions and successional strategies of the early-successional birch and the late-successional fir affected treeline dynamics by combining plot data with an individual-based treeline model at Himalayan treelines. Fir showed increasing recruitment and a higher upslope shift rate (0.11 ± 0.02 m y^{-1}) compared to birch (0.06 ± 0.03 m y^{-1}) over the last 200 years. Spatial analyses indicated strong interspecies competition when trees were young. Model outputs from various climatic scenarios indicate that fir will likely accelerate its upslope movement with warming while birch recruitment would decline drastically, forming stable or even retreating treelines. Our findings point to accelerating successional dynamics with late-successional species rapidly outcompeting pioneer species, offering insight into future forest succession and its influences on ecosystem services.

Key words: climatic warming, succession, Himalayas, interspecies interactions, treeline dynamics.

1. Introduction

Understanding the processes and mechanisms that determine species coexistence and succession is a fundamental ecological challenge[1]. Spatiotemporal changes in community composition in response to environmental variability are crucial yet insufficiently understood components of vegetation dynamics, particularly in mixed forests[2,3]. A special case in this regard are tree communities located at their climatic distribution limits where temperature and/or drought stress is high, the establishment rate is low, and several abiotic and biotic factors co-determine tree-to-tree interactions[4]. Interactions between tree species can benefit forest productivity and modify ecological succession by enhancing resource use efficiency to minimize the impacts of harsh climatic conditions on trees[5,6]. At the same time, the spatial distribution patterns of tree species reflect their ability to withstand adverse environmental conditions and provide insights into their interactions and processes, including dispersal, regeneration, competition, survival, and growth[7-9].

Climate-driven alpine treelines are among the most sensitive terrestrial ecosystems due to the extreme climatic conditions and a short growing season[10]. Alpine treelines are thus considered natural indicators to monitor the impacts of a warming climate on the structure and function of mountain ecosystems[9,11]. Climatic warming is expected to enhance tree growth and recruitment, and thus favors an upward expansion of treelines[12-16]. The responses of treelines to climatic warming at the global scale, however, are heterogenous and differ among sites or species, depending on treeline compositions[17-20]. This variability indicates that non-climatic factors such as intra- and interspecific interactions and microsite features influence treeline dynamics[13,15,21-23].

Species interactions mediated by climatic factors affect ecosystem functions[24]. For instance, facilitative effects among neighboring plants in harsh environments may ameliorate microclimatic conditions and enhance resource allocation that benefits the establishment and survival of tree recruits[5,25]. In contrast, competition between neighboring recruits may reduce their growth and resource acquisition, which in turn increases their mortality rate[11]. As such, the functioning of coexisting tree species is driven by species-specific successional strategies or traits[26,27], whereby species succession is strongly accelerated by climatic warming[28]. In general, fast-growing, early-successional broadleaf species show a lower drought resistance than slow-growing, late-successional species and may be more vulnerable to warming-induced moisture stress[29,30]. Interspecific competition is thus considered a crucial factor that determines forest structure by influencing the establishment, growth, and survival of new recruits[26,31]. Species with a higher growth potential under climatic warming are likely to outcompete stress-intolerant species with a lower growth potential[23,32-34]. Studying successional dynamics in forests and at treelines is challenging due to the long lifespan of trees, but analyzing the distribution of stand age and spatial patterns of trees can offer valuable insights into successional dynamics[35]. The influences of intra- and interspecific interactions and successional strategies on the shift rates of mixed treelines under climatic warming remain unknown, despite their crucial role in influencing mountain ecosystems.

The central Himalayas are among the largest and most continuous areas of alpine treelines in the world [12]. These treelines are dominated by the early-successional Himalayan birch (*Betula utilis*), the late-successional Himalayan fir (*Abies spectabilis*), or both. Himalayan mountain ecosystems rank among the most rapidly warming ecosystems in the world and are highly sensitive model areas to study climate change impacts[36,37]. Recent studies have shown that the response of tree growth to climate in treeline ecotones is species-specific, exemplified by the sensitivity of birch to moisture[37,38], and the sensitivity of fir to temperature[38,39]. Increasing tree recruitment and the upslope movement of Himalayan treelines have been consistently observed with warming[12,40]. However, these rates also depended on precipitation during early growing season[12] or intraspecies interactions[21]. Comparatively little is known about how climatic change drives Himalayan fir and birch range limits by modulating species interactions and succession at mixed treelines.

This study examined how climatic warming has affected recruitment patterns and treeline shifts of early- and late-successional tree species in the central Himalayas. By combining field observations with an individual-based treeline model, we aimed to answer whether species interactions and successional strategies are influencing shift of the early- and late-successional species under continued climatic warming. Despite early successional species typically establishing in open areas, due to the divergent climate sensitivity and successional strategies of the two species, we anticipated that fir would advance uphill more rapidly by outcompeting birch. To test this hypothesis, we explored three Shared Socio-Economic Pathway (SSP) scenarios of future climatic changes and their influence on successional dynamics in mixed treelines.

2. Results

2.1. Recruitment patterns and treeline dynamics

Recruitment patterns differed between the two study tree species. Fir showed increasing recruitment in recent decades, whereas the highest recruitment peak for birch was found between the 1920s and the 1970s, with a lower recruitment rate in recent decades (Fig. 1a). Decadal recruitment patterns did not significantly differ between plots at the intraspecific level but did it at the interspecific level (Kolmogorov-Smirnov tests, plot E1, D = 0.44; plot E2, D = 0.56; plot M1, D = 0.26; $P < 0.05$).

Both fir and birch treelines shifted upslope but at different rates. The rate over the last 200 years was much higher for fir than birch (0.11 ± 0.02 vs 0.06 ± 0.03 m y^{-1}; $t = 2.16$, $P < 0.05$) (Fig. 1b-d).

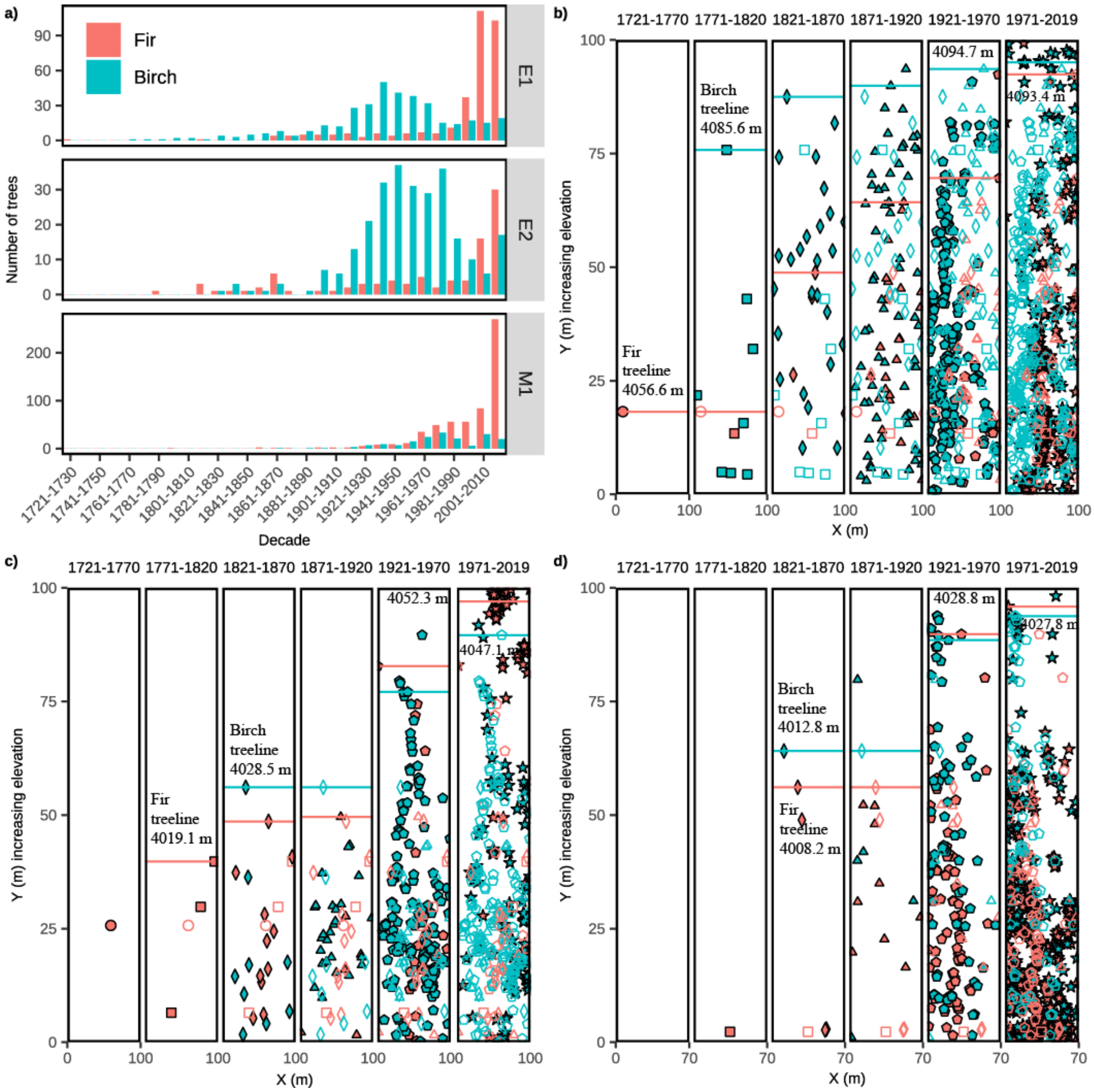

Fig. 1. Long-term variation in decadal tree recruitment in the mixed treeline plots sampled in the central Himalayas (a) and spatiotemporal changes in tree and treeline position in the three treeline plots (E1, Everest plot 1; E2, Everest plot 2; and M1, Manang plot 1) located in the central Himalayas (b-d). Treeline elevation is indicated by a horizontal line when tree height is > 2 m. Each solid symbol represents a tree recruited in the period indicated at the top of each plot, whereas hollow symbols represent living trees germinated in previous periods. Cyan and red symbols and lines represent birch and fir, respectively. X and Y represent horizontal and vertical distances from the left bottom corner (x, y = 0, 0) of the plot, respectively.

2.2. Spatial patterns: Intra- and interspecific interactions

The establishment of both species indicated conspecific associations (Fig. S1). The intraspecific univariate analysis of point patterns of two age classes indicated clustered spatial patterns among young trees (age < 50 years) for both species at all sites at spatial scales from 1 to 6 m (goodness-of-fit tests, GoF, $P < 0.05$). By contrast, old trees (age ≥ 50 years) showed random distribution patterns except old birches in plots E1 and E2 (Fig. S2). Most of the bivariate analyses between the two age classes indicated random spatial distributions (Fig. S3).

At the interspecific level, spatial segregation was detected between the young and old fir and birch individuals in all plots (Fig. 2). In plot E1, a strong segregation was observed between young fir trees and both young (up to 26 m) or old birch trees (up to 30 m) (GoF, $P < 0.001$). Similarly, adult fir and young birch trees were segregated at spatial scales of 1-2 and 4-9 m (GoF, $P < 0.001$), whereas adult fir and birch trees were also segregated at scales of 1-7 and 22-23 m. Young fir and birch trees in plot E2 were negatively associated at spatial scales of 3-7 m, whereas young fir and adult birch trees were spatially segregated up to 10 m. Adult fir and young birch trees were also segregated at spatial scales of 1, 3-4 and 6-7 m, and adult fir and birch trees did not show significant spatial interactions. Young fir and birch trees in plot M1 were also negatively associated at spatial scales of 1-12 m, whereas young fir and adult birch trees were spatially segregated up to 30 m, and adult fir and birch trees were also spatially segregated at 3-9 and 15-17 m.

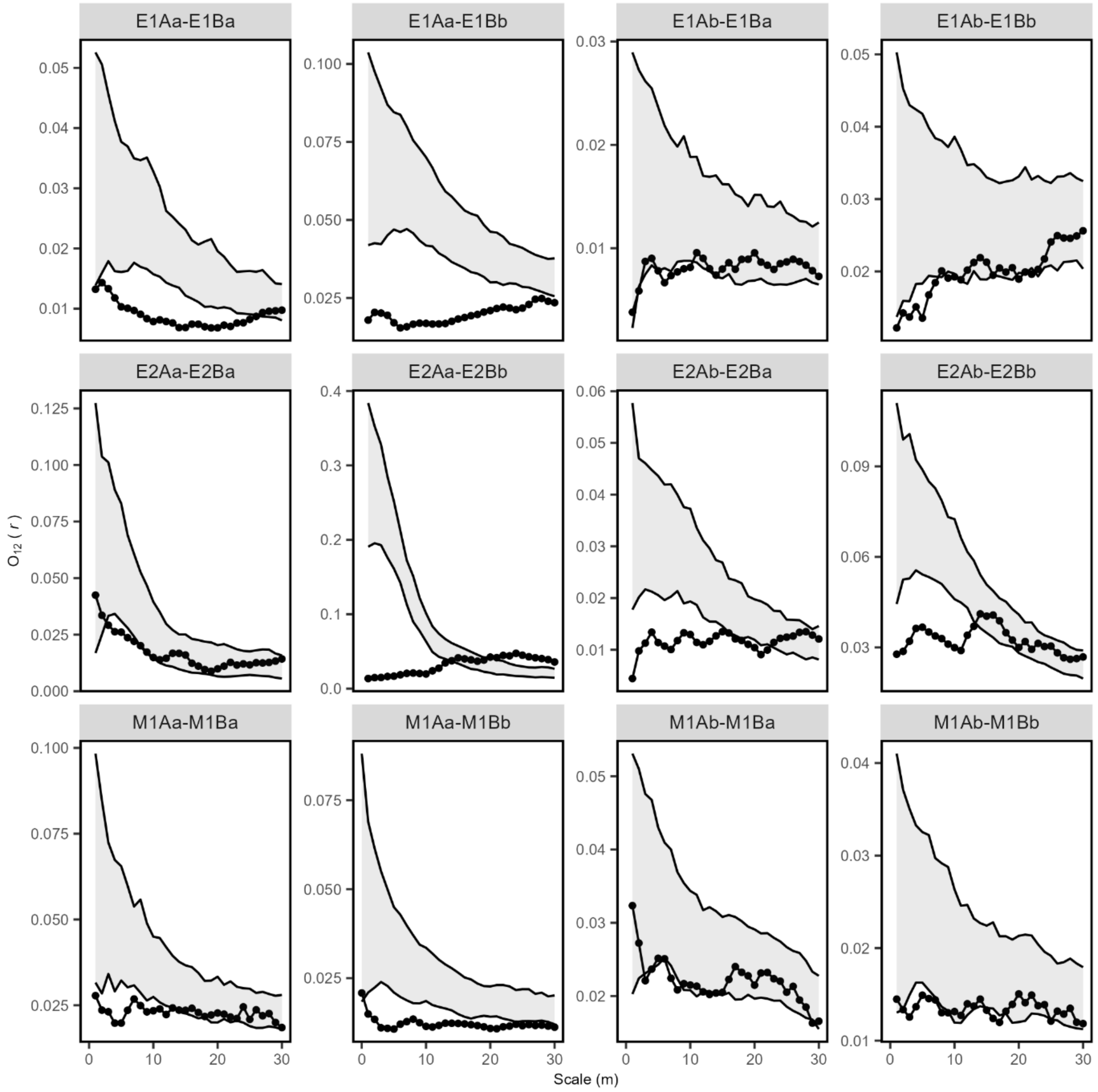

Fig. 2. Bivariate analysis of spatial point patterns for young and old birch and fir trees based on the bivariate O_{12} (r)-ring statistic. The continuous lines represent the upper and lower 99% simulation envelopes. Lines with symbols represent the O_{12} (r)-ring statistics calculated at different spatial scales (x-axes), and values beyond the upper and lower envelopes indicate significant ($P < 0.01$) aggregation and repulsion, respectively. E1, Everest plot 1; E2, Everest plot 2; and M1, Manang plot 1; A, fir; B, birch; a, age < 50 years; b, age ≥ 50 years. The distances were calculated from firs to birches and old trees to young trees.

2.3 Simulated treeline dynamics

We simulated changes in tree density and treeline dynamics under three SSP scenarios (SSP126, SSP370, and SSP585) during 2015-2100 to forecast the responses of treelines to increasingly warmer conditions. Firstly, we found that fir responded better than birch to both warmer and drier conditions (Figs. S4, S5). Secondly, the simulations indicated that birch was the first colonizing species forming a treeline, and then fir started to colonize 21 years later. Stable treelines formed in all scenarios after 50 annual simulations. Fir treelines advanced rapidly with increasing warming, whereas birch treelines were stable or even receded during the last 50 years (Figs. 3, 4).

Climatic warming continuously accelerated the advance of fir treelines, whereas birch treelines initially advanced and then retreated after reaching a peak shift rate in the SSP126 climatic scenario. During the spin-up period (stabilization phase), birch density consistently remained higher than fir density (Fig. S6). Under SSP585, the density of adult birch trees in the plots increased rapidly during the first 50 years and then gradually stabilized or even declined. The adult density of both species decreased with increasing warming rates in the considered SSP scenarios. However, changes in adult density differed between the two species ($P < 0.001$) under all scenarios with the upward shift rate of fir accelerating in response to warmer SSP scenarios (Fig. 4).

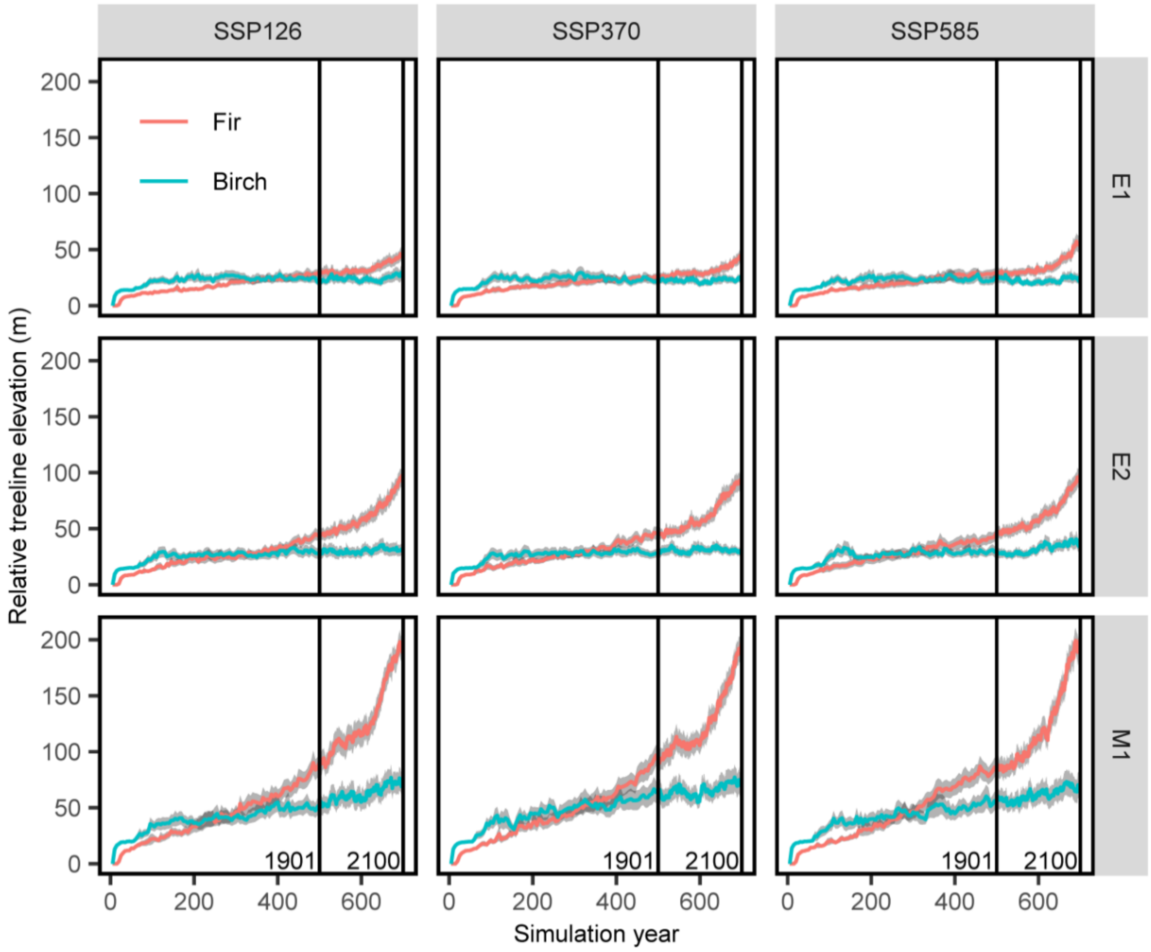

Fig. 3. Simulated relative treeline elevation changes (n = 50) of birch and fir for the E1, E2 and M1 plots including projected temperature and precipitation under three SSP scenarios (SSP126, SSP370, and SSP585). During the first 50 years of spin-up, 200 seeds (100 birches and 100 firs) entered the plots every year. Various biotic and abiotic species-specific variables were considered in the model simulation (see Table S2 for detail). The treeline position is calculated as the uppermost elevation of individuals with tree height is > 2 m. The vertical lines represent the years 1901 and 2020 of the real simulation phase. The cyan and red lines represent birch and fir, respectively. Shaded grey areas around cyan and red lines represent the standard error.

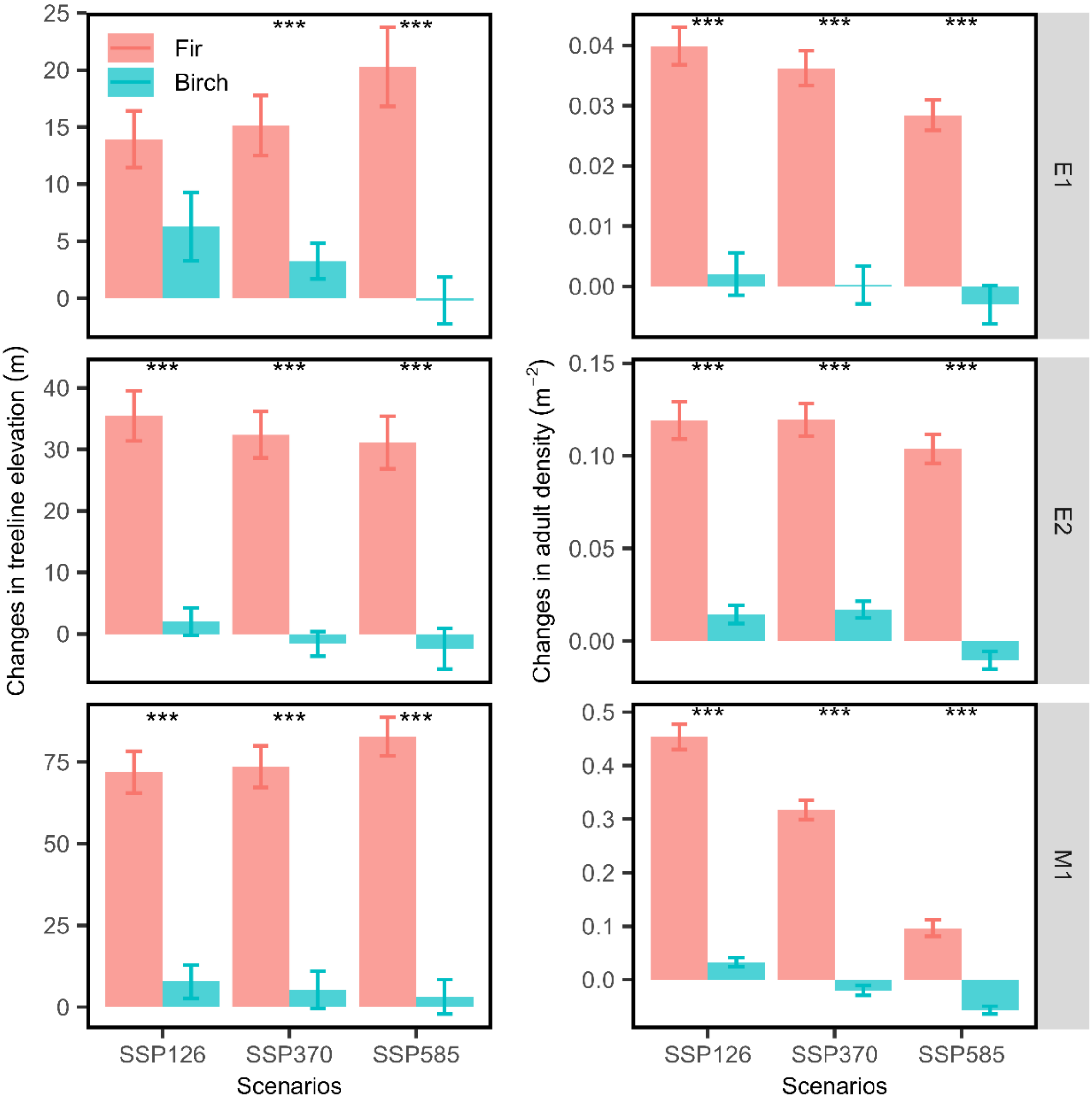

Fig. 4. Changes in treeline elevation (left panel) and adult (height > 2.0 m) tree density (right panel) of birch and fir under projected temperature and precipitation in three SSP scenarios (SSP126, SSP370, and SSP585) during 2015-2100 in the three study plots (E1, E2 and M1). The error bars represent standard errors. The cyan and red lines represent birch and fir, respectively. * $P < 0.05$, ** $P < 0.01$, and *** $P < 0.001$.

3. Discussion

The spatiotemporal patterns of tree recruitment at mixed treelines drive changes in their elevational position. Divergent recruitment patterns of fir (increasing) and birch (decreasing) were observed during the recent decades in response to climatic warming. Birch recruitment in the treeline ecotone has likely exceeded optimal climatic thresholds, as has been observed in other treelines in response to climatic warming and drying[20,41]. It is important to note, however, that the impacts of climatic stresses may partially be buffered by species interactions. This includes facilitation, which enhances tree establishment and protects recruits from harsh climatic conditions[5,21]. We identified increasing fir recruitment in recent decades, which indicates that fir is benefitting from the warming conditions[11,14,42]. Conversely, declining recruitment of the moisture-sensitive pioneer species birch could be caused by warming-induced moisture stress. This is in line with the results of studies on alpine shrublines[43], and alpine forbs and herbs[44] in the Himalayas. In addition, reduced birch recruitment suggests that factors other than temperature, such as biotic interactions, could limit establishment of seedlings as in other treelines[45,46]. Such interactions may intensify competition between tree species for favorable microsites, sunlight, soil nutrients and moisture. Therefore, further densification of fir is expected in the coming decades due to its superior physiological performance under warmer temperatures [38]. However, this response will depend on availability of microsites for fir regeneration and its interactions with shrubs[13].

Tree recruitment and survival are fundamental processes driving treeline dynamics. Increasing recruitment due to a warming climate will likely trigger upslope treeline shifts[13,17]. In comparison to birch, higher recruitment rates and upslope shifts in fir suggest a greater acclimation of this species to a warmer climate. Birch thus has a narrower thermal tolerance for reproductive success than fir. Late-successional fir can establish at shady sites[47,48], whereas the pioneer, early-successional birch establishes at open sites or along forest margins[21,39]. This is also supported by their establishment performance in response to light availability (Fig. S7). In addition, thick snow cover may hinder seedling recruitment[11]; however, a warm spring conditions could accelerate snowmelt and provide soil moisture in spring. Birch survival is highly dependent on the supply of water from melting snow during the early growing season[49]. Rapid warming and frequent pre-monsoon drought may thus increase soil moisture deficits with potential negative impacts on birch establishment. On the other hand, the increasing intensity of disturbances such as early snowmelt, snow fungi, insect outbreaks, landslides, avalanches, fires and hotter droughts will likely hinder the recruitment and survival of less resilient tree species[11].

The species-specific variations in recruitment and treeline shift rate may be due to their different responses to climate change. For instance, birch growth at treelines is mainly limited by low soil moisture availability in spring[37-39,50], whereas fir growth is enhanced by warming temperatures during the growing season[38,39]. Warmth-demanding species can readily colonize upwards, while others are struggling for survival under a warming climate and lagged shifts in range[27]. A higher upslope shift rate of late-successional fir compared to the early-successional birch indicates that fir will likely rapidly outcompete birch in response to projected future warming. As high Himalayan regions are warming and drying (Fig. S8), fir can overcome moisture stress thanks to its higher water-use efficiency[38]. By contrast, drought-induced xylem cavitation and production of very narrow or even missing growth rings in birch renders this species vulnerable to ongoing aridification[37,50]. The decoupling between temperature variability and range shifts of mountain vascular plants at the global scale[17,18,23] and diverse thermal thresholds for cambial reactivation between coexisting species at treelines[51] also support our findings. Likewise, controlled experiments have also suggested that range expanders outperformed pioneer native species in both normal and dry conditions[30].

The different spatial patterns at the intra- and interspecific levels and among age classes indicate that changes in the age and size structures of stands may also buffer the impacts of warming climatic conditions on treeline dynamics. Spatiotemporal variations in age are due to either distance- and/or density-dependent seed dispersal, seedling recruitment, growth, mortality[52,53], or to the availability of microsites that together determine the regeneration niche[45,54]. In addition, climatic stress and facilitation both affect the growth and survival of recruits at treelines[5,21]. Spatial patterns in such harsh environments mainly depend on competition for soil nutrients, water and temperature[55]. Conspecific aggregation (positive interactions) of young trees likely attenuates the negative impacts of resource limitation and climatic stress on their recruitment, growth and survival[5]. Shifts from clustered to random spatial distributions with increasing tree ages, however, result from stronger competition for light as succession advances[42,56]. This was further shown by the preferential establishment of birch seedlings in canopy gaps[21].

Strong competition between young trees, and random spatial patterns between young and old trees, despite conspecific clustering, imply that interspecific competition in recent decades has played an important role in determining treeline dynamics. Different recruitment patterns of tree species in mixed treelines are driven by interspecific competition in addition to climate. Birch is highly sensitive to competition for light and moisture[49]. In contrast, fir seedlings can establish and survive in more closed-sites[47]. The taller fir with larger crown coverage (Table S1) indicates that fir may pose a threat to the establishment of birch seedlings by shading sunlight if treeline ecotones rapidly encroach, as was observed in our model simulations (Fig. 4). These findings concur with the resource-ratio hypothesis of secondary succession[57]. The architecture of conifer crowns, however, is helpful for adapting to harsh environmental conditions, even though birch may also regenerate through sprouting[58]. Seed germination in early-successional species is strongly influenced by resource availability and competition, particularly in late-successional communities[33,59]. Due to the higher drought tolerance and water-use efficiency of late-successional fir compared to early-successional birch[38,60], the latter is likely to be rapidly outcompeted, if there are no significant disturbances in the coming years. Recently, it is well recognized that rapid climatic warming and biotic interactions are major drivers of ecological succession[61], as they alter the environmental filtering and dimension of plant-soil interactions[62]. Thus, despite declining recruitment of both species under higher SSP scenarios, the significant difference in treeline elevation and changes in adult density of the two study species during the real simulation period is likely due to accelerated warming-induced interactions, rather than a natural process. This has resulted in an increasing seedling establishment and the upslope shift rate of fir under past climate warming that will likely continue in the future. The shift of dominant plant functional types from deciduous to evergreen may also alter ecological functions such as the rate of litter decomposition, carbon and nitrogen cycling, water-use efficiency, interactions with animals and fungi, and energy fluxes[28], with further impacts on the composition of alpine plant communities[32].

4. Conclusions

Aiming to improve our limited understanding of changes in species interactions and their impacts on successional dynamics at mixed treelines, this study showed how warming accelerates succession and treeline shifts of fir, a late-successional species. Fir has been recruiting at a higher rate than birch and has moved upslope at a faster pace in recent decades. Fir is thus likely to outcompete birch at mixed treelines and is poised to becoming the dominant treeline species in the Himalayas. This trend is expected to continue under scenarios of future climate warming. The divergent patterns of tree recruitment and treeline shift rates of early- (birch) and late-successional (fir) species were mainly mediated by climate variability. The reconstructed fine-scale spatiotemporal patterns offer vital insights into the mechanisms driving ecological succession, such as species interactions and in community structure changes (species replacement or succession) over time. These insights enhance our ability to ecologically forecast the impacts of warming on alpine treeline ecotones. Our findings also shed light on the ecological threats of tree encroachment by switching from treelines dominated by deciduous broadleaves to others where evergreen conifers are the most abundant tree species.

5. Materials and methods

5.1. Study area

The study areas are located in the Sagarmatha (Mt. Everest) National Park and Annapurna Conservation Area (Manang), Nepal. Sagarmatha National Park is one of the world natural heritage sites listed by UNESCO and the oldest national park in high mountainous areas in Nepal. It extends from a temperate region (2445 m a.s.l.) to the top of the world, Mt. Everest (8848.86 m a.s.l.). Our sampling sites were located about 20 km southwest of Mt. Everest and about 10 km from the Pyramid meteorological station (5050 m a.s.l.). Climatic data from the Pyramid station indicated that this region had been characterized by warming and drying climatic conditions during recent decades (Fig. S8). The Manang Valley, situated within the Annapurna Conservation Area, is part of the trans-Himalayan region. This conservation area ranges from the subtropical region (at 790 m) above sea level to the peak of Mt. Annapurna I (at 8091 m) above sea level. The valley receives less precipitation than nearby areas due to the rain shadow effect of the Annapurna massif and has experienced increasing temperatures and declining precipitation in recent decades[12]. These regions are strongly influenced by the Indian summer monsoon with about 80% of rain falling during the summer.

5.2. Treeline plots and field sampling

Himalayan birch (*Betula utilis* D. Don) and Himalayan fir (*Abies spectabilis* (D. Don) Mirb.) are the dominant tree species across the central Himalayan treelines. Several valleys have pure stands of these species forming treelines, but some areas have mixed, conifer-broadleaf treeline ecotones (Fig. S9). However, if treeline is formed by birches, birch followed by fir within several meters. We selected sites that were far from settlements, minimizing negligible anthropogenic disturbances and were also away from landslide or avalanche areas. Both sampled tree species are unpalatable to livestock and wildlife. Two permanent 100 m × 100 m plots in the Everest region (E1; 4096 m and E2; 4054 m, north facing slope) and one 70 m × 100 m plot in Manang (M1; 4031 m, south-west facing slope) were established on a topographically uniform area (slope $< 20°$) of the mixed treeline (Fig. S10). Each plot contained the uppermost tree species line (upper limit of seedlings, height $<$ 0.5 m), the treeline (upper limit of trees 2 m tall) and the forest limit (upper limit of stands with tree covers $\geq 30\%$). The vertical side (y-axis) of each plot was set parallel to the elevational gradient, including the forest limit and the treeline[12-14]. The lower left corner of each plot was considered as the origin of a local coordinate system $(x, y) = (0, 0)$. The latitude, longitude and elevation of the upper and lower points of the plots were recorded to the nearest 0.1 m using GPS. The positions of all trees of the two target species within the plots were determined based on the (x, y) reference points, and the diameters at the base and at breast height (Dbh, measured at 1.3 m) and the crown diameters for all trees along the x and y directions were measured. Tree height was measured using a measuring stick if tree height was ≤ 2 m or using a clinometer if tree height was > 2 m. Average height and horizontal crown projections of the oldest age-classes (older than 100 years) were larger for fir than birch (Table S1). We did not find any cut stumps, dead trees or snags within the plots or beyond the current treelines and no fire scars were observed in the stems and tree-ring samples. Thus, existing trees were established during the last 200-300 years.

A core was collected from the base of each living tree with a Dbh > 5 cm using a Pressler increment borer to reconstruct the age structure of trees located within the plots (n = 216 birch trees and n = 141 fir trees). Cores were extracted as close to the ground as possible to minimize errors when estimating tree age. We also collected cores at a height of 2 m corresponding to the treeline definition (n = 22 birch trees and n = 20 fir trees) to estimate the changes in position of the treeline. The ages of seedlings and saplings (height < 2.5 m) were nondestructively estimated by counting bud scars and internodes along the main stem[13,14]. Basal wood cross-sections of the seedlings (n = 9 birch and n = 7 fir) were also collected to validate the age estimates. Estimated ages of fir were very close (± 1.5 years), while birch ages were overestimated by about 4 years to their germination dates[12]. All cores were processed and analyzed using standard dendrochronological methods including mounting, sanding and cross-dating. If the pith was missing from the cores, pith offset was calculated by applying a geometric pith-locator method[63] and was corrected using age-height relationship if coring was not possible close to the ground. Germination dates of the sampled trees were assigned, and age-diameter relationships were then developed for both species and sites (Fig. S11). These relationships were used to estimate the ages of trees with a rotten/missing pith or trees that were not cored.

We reconstructed recruitment dynamics on a decadal scale for each species and site based on the age structure of the trees within the plots. We used a two-sample Kolmogorov-Smirnov test to compare the temporal patterns of tree regeneration between species and sampling site. The spatiotemporal variabilities of treeline position and tree density were calculated for 50-year intervals starting in 1721 and ending in 2021[12-14].

5.3. Analyses of spatial point patterns

To quantify the spatial interactions of Himalayan birch and Himalayan fir at treeline ecotones, point-pattern analyses were applied. We used the Wiegand-Moloney's O-ring statistic estimated using Programita software for univariate ($O_{11}(r)$) or bivariate ($O_{12}(r)$) point-pattern analysis[64]. This statistic is derived from the pair-correlation function ($g_{11}(r)$ or $g_{12}(r)$) and can distinguish between aggregation or overdispersion and attraction or repulsion in univariate and bivariate patterns, respectively. The $O_{11}(r)$ and $O_{12}(r)$ statistics were calculated at several scales or distances (r) based on the likelihood of density functions. Heterogeneous Poisson models for complete spatial randomness (CSR) were used as null models. We used smoothing algorithms based on kernel estimators to estimate the null models, because the intensity function affects heterogeneous Poisson processes. To correct for edge effects, we used a scale of 20 m for smoothing and set 30 m for the maximum scale of analysis.

The univariate $O_{11}(r)$ statistic was used to analyze the spatial patterns of two age classes [a, young class (age < 50 years), b, old class (age ≥ 50 years)], and the bivariate $O_{12}(r)$ statistic was used to analyze the spatial interactions between the age classes and tree species. We randomized the locations of young trees, keeping the locations of old trees fixed when calculating null models, assuming that old trees influence the location of young trees but not vice versa[64]. The distances were calculated from firs to birches. We calculated $O(r)$ statistics at 1-m resolution for both analyses and assessed the divergence of the patterns from CSR considering scales from 1 to 30 m. Simulation envelopes, which define the significance of observed univariate (random, aggregated or overdispersed) and bivariate (attraction, repulsion or independence) patterns were calculated. The data were compared with the upper or lower 99% simulation envelopes created from 999 Monte Carlo simulations. Finally, we also calculated a goodness-of-fit (GoF) test for assessing the significance of the overall spatial pattern[64].

5.4 Simulating treeline dynamics

We collected data for the occurrence of Himalayan birch (296 sites) and Himalayan fir (204 sites) in the Himalayas and surrounding mountains using Global Biodiversity Information

Facility (GBIF) database (https://www.gbif.org/) to obtain the ranges of temperature and moisture for these two species (Fig. S4). The occurrence data were filtered following the method by Kindt[65]. After removing duplicates, we only kept data with accurate elevation records for temperature interpolation. Monthly temperature and precipitation were derived from the CRU TS v4.07 data set (1901–2022) with a spatial resolution of 0.5° [66] due to a lack of long-term observed climatic data. Gridded climatic data were interpolated using the delta downscaling method[67] to obtain site-specific data set of temperature and precipitation near the treelines. The interpolated temperature and precipitation align well with the observed data at treeline ecotones[53]. The ‘SPEI’ package (v. 1.7)[68] was used to calculate potential evapotranspiration (PET) based on the Thornthwaite and Mather[69] method which is widely used in individual-based forest gap models[53,70] and allowed us to identify a distribution range of species adapted to an annual degree-days (*uDD*)[70] and to a drought index:

$$uDD = \sum_{m=Jan}^{Dec} \max(T_m - kDTT,\ 0) \times kDays \ (1)$$

where T_m is the monthly temperature from January to December, *kDTT* is the threshold temperature of degree-days, which was >0 ºC in this model, and *kDays* is 30.5. The drought index is the ratio between yearly PET and precipitation, i.e. PET/P.

On this basis, we used a modified individual-based treeline model, the “Sygera Treeline Model”[53] to simulate treeline dynamics under various climatic scenarios (SSP126, SSP370, and SSP585). The species-specific biotic (competition, growth, seed production and dispersal, germination and mortality) and abiotic parameters were used in the model simulation under various scenarios of future climatic changes (see Table S2, Fig. S12 and model description in SI for details).

Birch and fir exhibited contrasting performance in the model due to their distinct growth patterns and environmental adaptations. Fir demonstrated faster growth and greater height potential compared to birch, supported by its higher maximum tree diameter increment, maximum tree height, and maximum diameter at breast height (Table S2). Additionally, fir showed superior adaptation to warmer and drier conditions, resulting in higher growth rates under simulated warming scenarios. Finally, given their shade-intolerant and shade-tolerant traits respectively, birch and fir were subjected to different light availability functions in our model (*availableL*) on their establishment performance (f_{shadow})[70]:

$$f_{shadow} = \begin{cases} 1 - e^{-4.64(availableL - 0.05)}, & Fir\ (2) \\ 2.24 * (1 - e^{-1.136(availableL - 0.08)}), & Birch\ (3) \end{cases}$$

A 500-year spin-up (stabilization) phase was carried out for each simulation year to reach a stabilized initial state of the population dynamic before the real simulation. Annual climatic data for this period were randomly selected for 1901–1930 to force the model simulation. In the model, 200 seeds (100 birch and 100 fir) were randomly introduced on a hypothetical mountain slope every year for the first 50 years where the temperature gradually decreased with elevation and interacted with each other (Fig. S13). We then performed a real simulation using field data from 1901–2020. All trees passed through five stages (environmental update, seed production and dispersal, establishment, growth and mortality). Firstly, we updated the climatic variables and evaluated the competition index based on neighboring trees for each grid cell (0.5 m × 0.5 m). Secondly, adult trees (> 2 m height) produced seeds that were coupled with tree size[71] and randomly dispersed based on seed-dispersal functions[72,73]. Thirdly, each seed germinated at a rate depending on the current abiotic and biotic conditions. Fourthly, the diameters measured at the base or at breast height (1.3 m) were used to represent radial growth. The actual increase in diameter was an optimal growth in diameter which was modified by environmental factors. Height and canopy size were calculated based on the current diameter.

Finally, the mortality rate was calculated for each tree, and dead trees were removed from the plot, based on the current environmental conditions and inherent mortality. We assumed that both the birch and fir treelines were in the center of the plot (i.e. at a relative elevation of 100 m) in 2020. We therefore trained the free parameters at all sites (E1, E2 and M1). We used the final value of each parameter after 5000 simulations.

We used projected temperature and precipitation data from three SSP scenarios computed in the Coupled Model Intercomparison Project Phase 6 (CMIP6) (https://data.isimip.org/) to simulate treeline dynamics (Table S3 and Fig. S14). Linear relationships between historical and projected climate data were established, based on the common period from 2015 to 2022. Temperature and precipitation data were corrected using historical data. From SSP126 to SSP585, there are increasing warming rates; however, precipitation shows negligible changes with only slight increases in SSP585 (Table S3). These data were successfully used in climatological study in this region and have reported similar patterns[74]. Historical data (1901-2022, derived from the CRU TS v4.07) was interpolated using the delta downscaling method[67] to obtain site-specific monthly temperature and precipitation. Projected monthly temperature and precipitation (2015-2100) were derived from multiple models (CanESM5, CESM2-WACCM, EC-Earth3, GFDL-ESM4, IITM-ESM, IPSL-CM6A-LR, KACE-1-0-G, MIROC6, and TaiESM1). The model was operated under three SSP scenarios (SSP126, SSP370, and SSP585) during 2015-2100. The dynamics of the birch and fir treelines and adult density were simulated for each warming scenario across all three sites with 50 replications. All the analysis, except for point pattern analysis, were performed in R 4.3.1[75].

Data availability

The CRU TS v4.07 climate dataset was obtained from https://crudata.uea.ac.uk/cru/data/hrg/. The SSP scenarios in the CMIP6 were downloaded from https://data.isimip.org/. Data were achieved in the National Tibetan Plateau Data Center: https://doi.org/10.11888/Terre.tpdc.301173.

Code availability

Statistical analysis in this study was performed with publicly available packages in R (version 4.3.1)[75] and Progamita software (https://programita.org/)[64]. The custom codes for the analysis of the data and the modified Sygera Treeline Model were archived in the National Tibetan Plateau Data Center: https://doi.org/10.11888/Terre.tpdc.301173.

Acknowledgements

This work was supported by the National Natural Science Foundation of China (42030508, 41988101) and the Second Tibetan Plateau Scientific Expedition and Research Program (STEP) (2019QZKK0301). J. Peñuelas was supported by the Spanish Government grants PID2022-140808NB-I00, and TED2021-132627 B–I00 funded by MCIN, AEI/10.13039/ 501100011033 European Union Next Generation EU/PRTR, the Fundación “Ramón Areces” grant CIVP20A6621, and the Catalan Government grants SGR 2021–1333 and AGAUR2023 CLIMA 00118. J.J.C. acknowledges funding by Spanish Ministry of Science and Innovation projects PID2021-123675OB-C43 and TED2021-129770B-C21. The Department of National Parks and Wildlife Conservation, Government of Nepal, is especially acknowledged for granting research permission. We thank Samresh Rai and Satyam Chaudhari for their help during the fieldwork and Yutong Zhao for data analysis.

Author contributions

E.L. designed the research; S.R.S. and J. Pandey collected data; S.R.S. and Z.X. analyzed data; S.R.S. drafted the paper with intensive input from E.L., F.B., J.J.C. and J. Peñuelas. All authors contributed ideas, interpreted the results and were involved in the editing and writing of the paper.

Competing interests

The authors declare no competing interests.

References

1. Levin, S. A. The problem of pattern and scale in ecology: the Robert H. MacArthur award lecture. *Ecology* **73**, 1943-1967 (1992).
2. Prach, K. & Walker, L. R. Four opportunities for studies of ecological succession. *Trends Ecol. Evol.* **26**, 119-123 (2011).
3. Collins, C. G. *et al.* Global change re‐structures alpine plant communities through interacting abiotic and biotic effects. *Ecol. Lett.* **25**, 1813-1826 (2022).
4. Kraft, N. J. *et al.* Community assembly, coexistence and the environmental filtering metaphor. *Funct. Ecol.* **29**, 592-599 (2015).
5. Callaway, R. M. *et al.* Positive interactions among alpine plants increase with stress. *Nature* **417**, 844-848 (2002).
6. Sanczuk, P. *et al.* Competition mediates understorey species range shifts under climate change. *J. Ecol.* **110**, 1813-1825 (2022).
7. Koffel, T., Daufresne, T. & Klausmeier, C. A. From competition to facilitation and mutualism: a general theory of the niche. *Ecol. Monogr.* **91**, e01458 (2021).

8. McIntire, E. J. & Fajardo, A. Beyond description: the active and effective way to infer processes from spatial patterns. *Ecology* **90**, 46-56 (2009).
9. Dial, R. J., Maher, C. T., Hewitt, R. E. & Sullivan, P. F. Sufficient conditions for rapid range expansion of a boreal conifer. *Nature* **608**, 546-551 (2022).
10. Camarero, J. J. *et al.* Global fading of the temperature–growth coupling at alpine and polar treelines. *Glob. Change Biol.* **27**, 1879-1889 (2021).
11. Körner, C. *Alpine treelines: functional ecology of the global high elevation tree limits*. Springer Science & Business Media, Basel, Switzerland (2012).
12. Sigdel, S. R. *et al.* Moisture-mediated responsiveness of treeline shifts to global warming in the Himalayas. *Glob. Change Biol.* **24**, 5549-5559 (2018).
13. Liang, E. *et al.* Species interactions slow warming-induced upward shifts of treelines on the Tibetan Plateau. *Proc. Natl Acad. Sci.* **113**, 4380-4385 (2016).
14. Camarero, J. J. & Gutiérrez, E. Pace and pattern of recent treeline dynamics: response of ecotones to climatic variability in the Spanish Pyrenees. *Clim. Change* **63**, 181-200 (2004).
15. Elliott, G. P. Influences of 20th-century warming at the upper tree line contingent on local-scale interactions: evidence from a latitudinal gradient in the Rocky Mountains, USA. *Glob. Ecol. Biogeogr.* **20**, 46-57 (2011).
16. Penuelas, J. & Boada, M. A global change ‐ induced biome shift in the Montseny mountains (NE Spain). *Glob. Change Biol.* **9**, 131-140 (2003).
17. Harsch, M. A., Hulme, P. E., McGlone, M. S. & Duncan, R. P. Are treelines advancing? A global meta ‐ analysis of treeline response to climate warming. *Ecol. Lett.* **12**, 1040-1049 (2009).
18. Lu, X., Liang, E., Wang, Y., Babst, F. & Camarero, J. J. Mountain treelines climb slowly despite rapid climate warming. *Glob. Ecol. Biogeogr.* **30**, 305-315 (2021).

19. Sharma, S. *et al.* North American tree migration paced by climate in the West, lagging in the East. *Proc. Natl Acad. Sci.* **119**, e2116691118 (2022).

20. Ali, M. *et al.* Contrasting treeline dynamics of pine and birch in response to climate warming in the Karakoram. *Trees* **36**, 1923-1932 (2022).

21. Sigdel, S. R., Liang, E., Wang, Y., Dawadi, B. & Camarero, J. J. Tree-to-tree interactions slow down Himalayan treeline shifts as inferred from tree spatial patterns. *J. Biogeogr.* **47**, 1816-1826 (2020).

22. Bader, M. Y. *et al.* A global framework for linking alpine-treeline ecotone patterns to underlying processes. *Ecography* **44**, 265-292 (2021).

23. Gallou, A. *et al.* Diurnal temperature range as a key predictor of plants' elevation ranges globally. *Nat. Commun.* **14**, 7890 (2023).

24. Tylianakis, J. M., Didham, R. K., Bascompte, J. & Wardle, D. A. Global change and species interactions in terrestrial ecosystems. *Ecol. Lett.* **11**, 1351-1363 (2008).

25. He, Q., Bertness, M. D. & Altieri, A. H. Global shifts towards positive species interactions with increasing environmental stress. *Ecol. Lett.* **16**, 695-706 (2013).

26. Kunstler, G. *et al.* Plant functional traits have globally consistent effects on competition. *Nature* **529**, 204-207 (2016).

27. Rumpf, S. B. *et al.* Extinction debts and colonization credits of non-forest plants in the European Alps. *Nat. Commun.* **10**, 4293 (2019).

28. Mekonnen, Z. A., Riley, W. J., Randerson, J. T., Grant, R. F. & Rogers, B. M. Expansion of high-latitude deciduous forests driven by interactions between climate warming and fire. *Nat. Plants* **5**, 952-958 (2019).

29. Dulamsuren, C. *et al.* Hydraulic architecture and vulnerability to drought-induced embolism in southern boreal tree species of Inner Asia. *Tree Physiol.* **39**, 463-473 (2019).

30. Yang, Q. *et al.* Temporal dynamics of range expander and congeneric native plant responses during and after extreme drought events. *Ecol. Monogr.* **92**, e1529 (2022).

31. Lyu, S. & Alexander, J. M. Competition contributes to both warm and cool range edges. *Nat. Commun.* **13**, 2502 (2022).

32. Wang, X. *et al.* Enhanced habitat loss of the Himalayan endemic flora driven by warming-forced upslope tree expansion. *Nat. Ecol. Evol.* **6**, 890-899 (2022).

33. Cantera, I. *et al.* The importance of species addition 'versus' replacement varies over succession in plant communities after glacier retreat. *Nat. Plants* **10**, 256-267 (2024).

34. Meng, Y., Li, S.-p., Wang, S., Meiners, S. J. & Jiang, L. Scale-dependent changes in ecosystem temporal stability over six decades of succession. *Sci. Adv.* **9**, eadi1279 (2023).

35. Johnson, E. A. & Miyanishi, K. Testing the assumptions of chronosequences in succession. *Ecol. Lett.* **11**, 419-431 (2008).

36. IPCC. Climate Change 2022: *Impacts, Adaptation, and Vulnerability*. Contribution of Working Group II to the Sixth Assessment Report of the Intergovernmental Panel on Climate Change. Cambridge, UK and New York, USA (2022).

37. Liang, E., Dawadi, B., Pederson, N. & Eckstein, D. Is the growth of birch at the upper timberline in the Himalayas limited by moisture or by temperature? *Ecology* **95**, 2453-2465 (2014).

38. Pandey, S., Cherubini, P., Saurer, M., Carrer, M. & Petit, G. Effects of climate change on treeline trees in Sagarmatha (Mt. Everest, Central Himalaya). *J. Veg. Sci.* **31**, 1144-1153 (2020).

39. Gaire, N. P., Koirala, M., Bhuju, D. R. & Carrer, M. Site- and species-specific treeline responses to climatic variability in eastern Nepal Himalaya. *Dendrochronologia* **41**, 44-56 (2017).

40. Chhetri, P. K. & Cairns, D. M. Contemporary and historic population structure of *Abies spectabilis* at treeline in Barun valley, eastern Nepal Himalaya. *J. Mt. Sci.* **12**, 558-570 (2015).

41. Bailey, S. N., Elliott, G. P. & Schliep, E. M. Seasonal temperature–moisture interactions limit seedling establishment at upper treeline in the Southern Rockies. *Ecosphere* **12**, e03568 (2021).

42. Wang, Y. *et al.* Increased stem density and competition may diminish the positive effects of warming at alpine treeline. *Ecology* **97**, 1668-1679 (2016).

43. Sigdel, S. R. *et al.* No benefits from warming even for subnival vegetation in the central Himalayas. *Sci. Bull.* **66**, 1825-1829 (2021).

44. Dolezal, J. *et al.* Vegetation dynamics at the upper elevational limit of vascular plants in Himalaya. *Sci. Rep.* **6**, 24881 (2016).

45. Batllori, E., Camarero, J. J., Ninot, J. M. & Gutiérrez, E. Seedling recruitment, survival and facilitation in alpine *Pinus uncinata* tree line ecotones. Implications and potential responses to climate warming. *Glob. Ecol. Biogeogr.* **18**, 460-472 (2009).

46. Tingstad, L., Olsen, S. L., Klanderud, K., Vandvik, V. & Ohlson, M. Temperature, precipitation and biotic interactions as determinants of tree seedling recruitment across the tree line ecotone. *Oecologia* **179**, 599-608 (2015).

47. Mainali, K. *et al.* Contrasting responses to climate change at Himalayan treelines revealed by population demographics of two dominant species. *Ecol. Evol.* **10**, 1209-1222 (2020).

48. Stainton, J. D. A. *Forests of Nepal* (181 pp.). John Murray. London, U. K. (1972).

49. Shrestha, B. B., Ghimire, B., Lekhak, H. D. & Jha, P. K. Regeneration of treeline birch (*Betula utilis* D. Don) forest in a trans-Himalayan dry valley in central Nepal. *Mt. Res. Dev.* **27**, 259-267 (2007).

50. Li, X., Rossi, S., Sigdel, S. R., Dawadi, B. & Liang, E. Warming menaces high-altitude Himalayan birch forests: Evidence from cambial phenology and wood anatomy. *Agric. For. Meteorol.* **308-309**, 108577 (2021).

51. Li, X. *et al.* Warming-induced phenological mismatch between trees and shrubs explains high-elevation forest expansion. *Natl Sci. Rev.* **10**, nwad182 (2023).

52. Murphy, S. J., Wiegand, T. & Comita, L. S. Distance‐dependent seedling mortality and long‐term spacing dynamics in a neotropical forest community. *Ecol. Lett.* **20**, 1469-1478 (2017).

53. Zheng, X. *et al.* Density-dependent species interactions modulate alpine treeline shifts. *Ecol. Lett.* **27**, e14403 (2024).

54. Bürzle, B. *et al.* Seedling recruitment and facilitation dependence on safe site characteristics in a Himalayan treeline ecotone. *Plant Ecol.* **219**, 115-132 (2018).

55. Körner, C. & Paulsen, J. A world‐wide study of high altitude treeline temperatures. *J. Biogeogr.* **31**, 713-732 (2004).

56. Yang, X. *et al.* Net plant interactions are highly variable and weakly dependent on climate at the global scale. *Ecol. Lett.* **25**, 1580-1593 (2022).

57. Tilman, D. The Resource-Ratio Hypothesis of Plant Succession. *Am. Nat.* **125**, 827-852 (1985).

58. Xu, C. *et al.* Enhanced sprout-regeneration offsets warming-induced forest mortality through shortening the generation time in semiarid birch forest. *For. Ecol. Manag.* **409**, 298-306 (2018).

59. Bazzaz, F. A. The Physiological Ecology of Plant Succession. *Annu. Rev. Ecol.Syst.* **10**, 351-371 (1979).

60. Panthi, S., Fan, Z.-X., van der Sleen, P. & Zuidema, P. A. Long-term physiological and growth responses of Himalayan fir to environmental change are mediated by mean climate. *Glob. Change Biol.* **26**, 1778-1794 (2020).

61. Chang, C. C. & Turner, B. L. Ecological succession in a changing world. *J. Ecol.* 107, 503-509 (2019).

62. Blois, J. L., Zarnetske, P. L., Fitzpatrick, M. C. & Finnegan, S. Climate change and the past, present, and future of biotic interactions. *Science* 341, 499-504 (2013).

63. Rozas, V. Tree age estimates in *Fagus sylvatica* and *Quercus robur*: testing previous and improved methods. *Plant Ecol.* **167**, 193-212 (2003).

64. Wiegand, T. & Moloney, K. A. *A Handbook of spatial point-pattern analysis in ecology*. Chapman and Hall/CRC, Boca Raton, Florida, USA (2014).

65. Kindt, R. TreeGOER: A database with globally observed environmental ranges for 48,129 tree species. *Glob. Change Biol.* 29, 6303-6318 (2023).

66. Harris, I., Osborn, T. J., Jones, P. & Lister, D. Version 4 of the CRU TS monthly high-resolution gridded multivariate climate dataset. *Sci. Data* **7**, 109 (2020).

67. Hay, L. E., Wilby, R. L. & Leavesley, G. H. A comparison of delta change and downscaled GCM scenarios for three mountainous basins in the United States. *J. Am. Water Res. As.* **36**, 387-397 (2000).

68. Beguería, S. & Vicente-Serrano, S. M. SPEI: calculation of the standardised precipitation-evapotranspiration index. *R package version* **1** (2017).

69. Thornthwaite, C. W. & Mather, J. R. Instructions and tables for computing potential evapotranspiration and the water balance. *Publications on Climatology* **10**, 185-311 (1957).

70. Bugmann, H. *On the ecology of mountainous forests in a changing climate: a simulation study*, ETH Zurich, (1994).

71. Greene, D. F. & Johnson, E. A. Estimating the mean annual seed production of trees. *Ecology* **75**, 642-647 (1994).

72. Kruse, S., Wieczorek, M., Jeltsch, F. & Herzschuh, U. Treeline dynamics in Siberia under changing climates as inferred from an individual-based model for *Larix*. *Ecol. Modell.* **338**, 101-121 (2016).

73. Vitali, A. *et al.* Pine recolonization dynamics in Mediterranean human-disturbed treeline ecotones. *For. Ecol. Manag.* **435**, 28-37 (2019).

74. Wang, T. et al. Atmospheric dynamic constraints on Tibetan Plateau freshwater under Paris climate targets. *Nat. Clim. Change* 11, 219-225, (2021).

75. R Development Core Team . R: *A Language and environment for statistical computing*. Vienna: R Foundation for Statistical Computing (2023).